Available online at www.sciencedirect.com
SCIENCE DIRECT®
Polymer 44 (2003) 6681–6688
polymer
www.elsevier.com/locate/polymer

Thermally- and solvent-induced crystallization kinetics of *syndiotactic* polystyrene viewed from time-resolved measurements of infrared spectra at the various temperatures (1) estimation of glass transition temperature shifted by solvent absorption

Akiko Yoshioka, Kohji Tashiro*

Department of Macromolecular Science, Graduate School of Science, Osaka University, Toyonaka, Osaka 560-0043, Japan

Received 4 February 2003; received in revised form 16 May 2003; accepted 15 July 2003

Abstract

syndiotactic Polystyrene (sPS) glass crystallizes into the α form when it is heated above the glass transition temperature (T_g, about 100 °C). sPS can be crystallized also into the δ form in the solvent atmosphere at room temperature. In order to trace the structural evolution process, the time-resolved infrared spectral measurements have been performed in the isothermal crystallization from the glass to α form and in the solvent-induced crystallization from the glass to δ form at the various temperatures. Absorbance of crystallization-sensitive infrared bands was plotted against time, from which the crystallization kinetics were analyzed on the basis of Avrami equation: $X(t) = 1 - \exp[-(kt)^n]$ where X is a normalized crystallinity, n is an index, k is a rate constant, and t is a time. The isothermal crystallization was investigated also by carrying out the temperature jump experiment of DSC thermograms, giving almost the same results as the infrared spectral measurements. The Avrami index n was 2–5 depending on the crystallization temperature (T_c). The k was also dependent on the T_c, about 10^{-1}–10^{-4} s^{-1} and could be fitted reasonably by the equation of crystallization kinetics. An extrapolation of the k vs T_c plot to the negligibly small k value allowed us to predict the temperature at which no crystallization should occur, ca. 100 °C, in good agreement with the observed T_g value. On the other hand, the solvent-induced crystallization was investigated for the first time at the various temperatures from 50 to 9 °C by the time-resolved measurement of infrared spectra. Compared with the experiment at room temperature, the crystallization was highly accelerated at 40–50 °C, while the crystallization rate was reduced remarkably at such a low temperature as 9 °C. The time dependence of infrared absorbance was analyzed for the crystallization-sensitive bands on the basis of Avrami equation as the first approximation, although the crystallization mechanism was more complicated than the isothermal crystallization case. The logarithm of the k value was found to change almost linearly with temperature and an extrapolation to infinitesimally small k value gave a T_g of about −15 °C. That is to say, the glass transition temperature was estimated to shift remarkably from 100 to −15 °C by absorbing solvent molecules or by a plasticizing effect.

Keywords: *syndiotactic* Polystyrene; Crystallization; Infrared spectra

1. Introduction

syndiotactic Polystyrene (sPS) shows a complicated polymorphism depending on the crystallization conditions. The amorphous glass, prepared by quenching the molten sample, crystallizes into δ form when it is exposed to the atmosphere of such organic solvent as benzene, toluene, etc. at room temperature [1–30]. In the δ form sPS chains take the $(TTGG)_2$ helical conformation and make a complex with solvent molecules. Rinsing the δ form in acetone or methanol gives the so-called empty δ_e form where the TTGG chains are packed in a similar crystal lattice with that of the original δ form but by keeping the vacant spaces originally occupied by solvent molecules [7,11,28,30]. When the δ form sample is heated, the solvent molecules evaporate and the γ form is obtained in which the TTGG chains are packed closely without any solvent included [3,6,12,17,18,26,29,30]. By heating at higher temperature the γ form transfers to the α form of all-*trans* zigzag conformation [26,31,32]. Heating of the glass sample above the glass transition temperature (T_g) of ca. 100 °C gives also the α form [32–40]. The α form is obtained also by cooling

* Corresponding author.

0032-3861/$ - see front matter © 2003 Elsevier Ltd. All rights reserved.
doi:10.1016/S0032-3861(03)00696-7

the molten sample to room temperature at relatively high rate, while the slow cooling of the melt results in the formation of the β form [41–47].

In spite of the publication of many papers about the polymorphism of sPS, the structural evolution in the crystallization and/or phase transition phenomena has not yet been clarified well because the in situ experiments during these phenomena were limited so far [10,19,21, 24–26,29–32,34,38,47]. In a series of papers [19,21,22,25, 29,30] we have studied the solvent-induced crystallization phenomenon of sPS glass by carrying out the time-resolved measurements of infrared and Raman spectra and X-ray diffraction, and clarified the structural evolution process in this crystallization phenomenon. The similar measurement was made also for the phase transitions from δ to γ and to α form in the heating process from room temperature [29,30]. In the analysis of infrared data we utilized a concept of critical sequence length [48] and investigated the regularization process of helical chain conformation from the microscopic point of view.

In this way we described the crystallization and phase transition behavior of sPS as a function of time, but we did not analyze the kinetics of the crystallization phenomena. The crystallization kinetics was investigated often by measuring DSC isotherms and the data were analyzed phenomenologically on the basis of Avrami equation [32, 38,47]. In order to relate such macroscopic data with the microscopically viewed structural change, we have carried out the time-resolved measurements of vibrational spectra and/or X-ray diffraction in the isothermal crystallization process and compared the results with the thermal data as will be reported in the present paper.

In the kinetics study, we investigated the two types of crystallization phenomenon. One was a thermally induced crystallization from the glass to the α form. Another one was a solvent-induced crystallization of the glass to the δ form. In the former case the experiment was made above T_g, while the latter case was below T_g. As for the thermally induced crystallization, the time-resolved measurement of infrared spectra was made in the *isothermal* crystallization process of the glass to the α form by carrying out the temperature jump experiment. In this case a key point for the successful measurement was how to make a sharp and stable temperature jump as will be described in a later section. The collected data were analyzed as a function of time and the crystallization kinetics were discussed on the basis of Avrami-type equation in comparison with the DSC data. As for the solvent-induced crystallization experiment, on the other hand, the time-resolved measurement of infrared spectra was made in the solvent atmosphere. The experimental results at room temperature were already reported in the previous papers [19,21,22,25,29,30]. The crystallization occurred even at room temperature, much lower than the original T_g of the sPS glassy sample. This is because the molecular motion of the amorphous chains is accelerated through the interaction between the polymer chains and the solvent molecules [19,21,22,25,29,30] or a plasticizing effect of absorbed solvent molecules. At this stage we need to answer the question: to what extent does the solvent shift the original T_g? One method to answer this question may be to measure the temperature dispersion of the dynamic viscoelastic property of the sPS glassy sample, but this experiment must be performed in an organic solvent atmosphere and is quite awful, although we reported this type of measurement in water vapor atmosphere [49–51]. It is rather easier for us to measure the infrared spectra for the sample set in a sealed optical cell, into which a solvent vapor is filled up. In the second part of the present paper we will describe the kinetic study of solvent-induced crystallization at the various temperatures on the basis of in situ time-resolved measurement of infrared spectra. The thus obtained data were analyzed quantitatively and the solvent-induced shift of T_g was estimated successfully.

2. Experimental

Samples. sPS samples (M_w 203,000, M_w/M_n 3.01) were supplied by Idemitsu Petrochemical Co. Ltd, Japan. Glassy samples were prepared by quenching the melt (280–300 °C) into ice water bath. The amorphous content was checked by infrared spectra.

DSC measurements. sPS was put into an aluminum pan and melted on a hot plate and then quenched into ice water. The sample pan was set into the DSC cell and the temperature was rapidly changed from 30 °C to the crystallization temperature at a rate of 500 °C/min with a Perkin Elmer Pyris 1 DSC apparatus.

Time-resolved infrared measurement in isothermal crystallization. In the time-resolved measurements of infrared spectra during the isothermal crystallization process, a homemade cell was used as shown in Fig. 1 [52]. sPS glass sample was set to a sample holder at room temperature. This holder was moved quickly to the metal plate (heater 1) kept at a predetermined temperature. The temperature was monitored by a thermocouple embedded in a sample. In order to increase the heating rate, another heater (heater 2) was set at almost the same time near the sample holder. The increasing rate of temperature was about 500 °C/min. The temperature was kept constant immediately after this jump. The infrared measurement was started before the jump and the spectral data were saved at a constant time interval (4–16 s depending on the crystallization rate). The infrared spectra were taken at a resolution power 2 cm^{-1} by using a Digilab (Bio-Rad) FTS-60A FT-IR spectrometer equipped with an MCT (mercury–cadmium-telluride) semiconductor detector.

The infrared spectral measurement was also performed during the slow heating process of the sPS glass. The sample was set in the heating cell and heated up step by step, during which the infrared spectra were measured.

Solvent-induced crystallization from glass to δ form. The

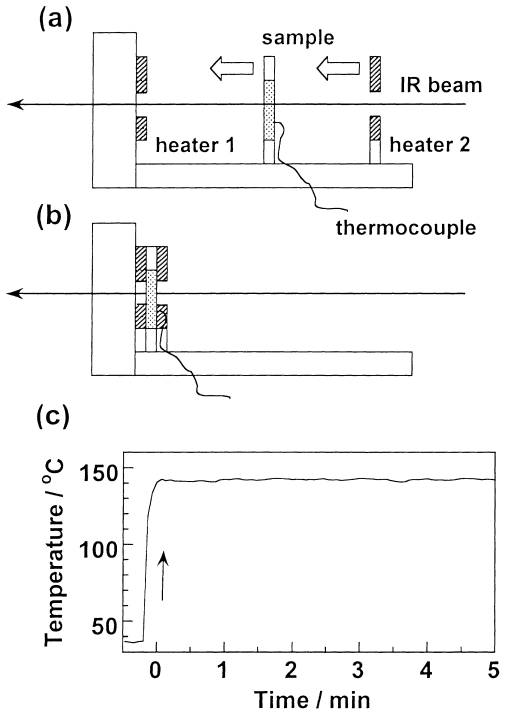

Fig. 1. An optical cell for the time-resolved infrared spectral measurements in the isothermal crystallization. (a) sPS glass sample was set to the sample holder at room temperature. The two heaters were kept at a crystallization temperature. (b) The sample holder and heater 2 were moved quickly to the metal plate (heater 1) and fixed during measurements. (c) The temperature change during the experiment was monitored by a thermocouple embedded in the sample.

time-resolved infrared spectral measurement was made also for the solvent-induced crystallization process. The optical cell with a solvent reservoir was used for the measurement, the details of which were reported in the previous papers [19,21,22,25,29,30]. A heater was attached to the walls of the cell for the high temperature measurements. The cell was cooled by ice-water bath when the measurement was made below room temperature. The temperature was monitored by a thermocouple contacted directly to the sample.

3. Results and discussion

3.1. Isothermal crystallization of the glassy sample

As mentioned in the introduction, when the amorphous sample is heated above T_g (ca. 100 °C), it crystallizes into the α form. In order to clarify the phenomenon microscopically, the infrared spectra were measured in the heating process as shown in Fig. 2. The temperature dependence of infrared absorbance is plotted in Fig. 3 for the bands characteristic of the amorphous phase and the α form. At room temperature, the bands characteristic of the amorphous sample were observed at 840, 970, 1195 and 1240 cm^{-1} and so on, and no crystalline band was observed.

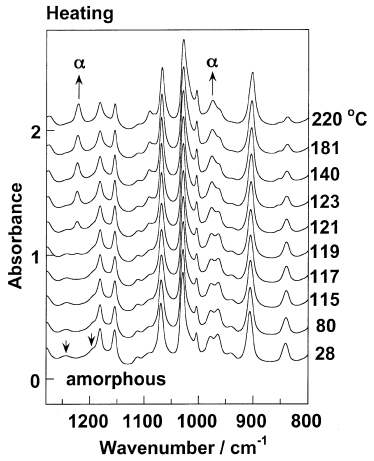

Fig. 2. Infrared spectra of sPS glass taken in the heating process from room temperature to 220 °C.

The spectrum did not change until the sPS glass was heated above 117 °C. At this point, some new bands started to be observed at 850, 980, 1090, 1222 and 1333 cm^{-1}, for example. They are assigned to the TT bands of the α form [22]. At the same time, the amorphous bands decreased in intensity. In the temperature region of 200–220 °C, the band intensity of the α form increased furthermore at higher rate, suggesting the regularization from the irregular α′ form to the regular α″ form [37]. A decrease in intensity of the α bands above 230 °C corresponds to the melting phenomenon of the α crystal.

The isothermal crystallization process was traced by carrying out the temperature jump experiments at 125, 139 and 152 °C (Fig. 3). Figs. 4 and 5 show the infrared spectral changes measured during the isothermal crystallization at 125 and 139 °C, respectively. The time dependence of band intensity is shown in Fig. 6 (125 °C) and Fig. 7 (139 °C). In both the cases, the amorphous bands became weaker with increasing time and the bands characteristic of the α form started to appear after some induction time. The induction time depended on the crystallization temperature: at 125 °C the induction time was about 1.5 min and at 139 °C it was only 5 s. The similar tendency could be seen also for the

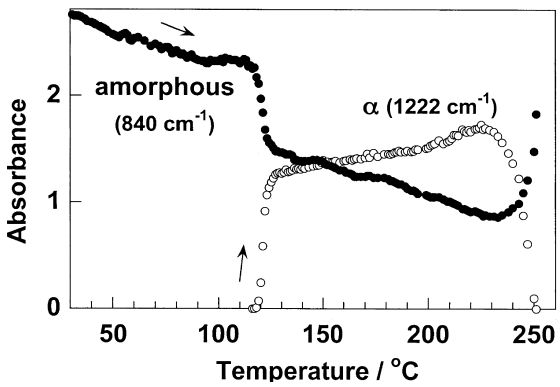

Fig. 3. Temperature dependence of infrared absorbance of the 840 cm^{-1} amorphous band and the 1222 cm^{-1} band intrinsic of the α form.

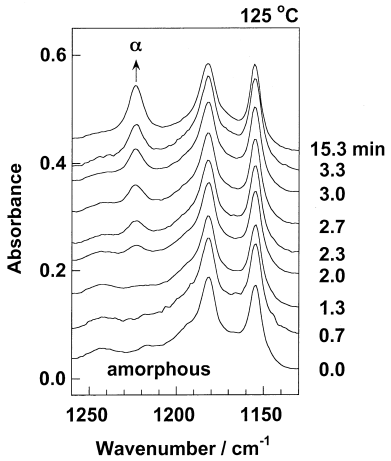

Fig. 4. Infrared spectral change of sPS glass during the isothermal crystallization at 125 °C.

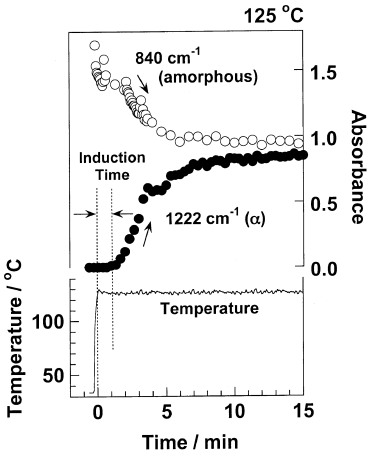

Fig. 6. Time dependence of infrared absorbance of the bands characteristic of the amorphous phase (840 cm^{-1}) and the α form (1222 cm^{-1}) measured in the isothermal crystallization at 125 °C. The absorbance of the amorphous band is shifted along the vertical axis for easier comparison.

crystallization rate or the slope of the absorbance-time curve as shown in Figs. 6 and 7: the increasing rate of infrared absorbance of the 1222 cm^{-1} α-form band was higher at 139 °C than 125 °C. We performed the similar experiments at temperatures quite close to T_g, about 110–120 °C, and found that the crystallization started in a time order of 10–20 min.

As reported in the previous paper [22], the α-form band at 1222 cm^{-1} has the critical sequence length of 30–40 monomeric units, i.e. this band can be detected for the first time when the regular zigzag chain grows its length to 15–20 repeating periods or ca. 100 Å, where one repeating period is about 5.0 Å. The 1333 cm^{-1} band has shorter m value (10–15 monomeric units). Unfortunately, it was impossible to detect any difference in observation timing between these two bands, suggesting that the regularization of a random coil to the planar-zigzag chain conformation of α form occurs too rapidly to trace the growing process at a high time resolution.

Fig. 8 shows the crystallization isotherms measured by DSC for the sPS glass sample at the various temperatures of 125, 130, 135 and 140 °C. The relative crystallinity was evaluated by integrating a heat output at a constant time interval. The induction time before the start of crystallization was almost equal to that estimated in the infrared measurement (Figs. 6 and 7). Fig. 9 shows the curves of double logarithm of the normalized crystallinity X plotted against a logarithm of time, or the so-called Avrami plot.

$$1 - X(t) = \exp[-(kt)^n] \quad (1)$$

$$\log[-\ln(1 - X)] = n \log k + n \log(t) \quad (2)$$

where $X(t)$ is the crystallinity at a time t, k is a rate constant and n is an Avrami index.

In this figure the experimental data collected for DSC and infrared spectra are compared with each other. In the infrared spectral analysis, the absorbance was normalized by using the value obtained after long crystallization time and was used as a normalized crystallinity X. These two

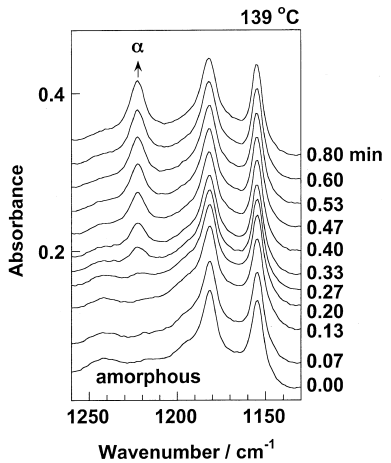

Fig. 5. Infrared spectral change of sPS glass during the isothermal crystallization at 139 °C.

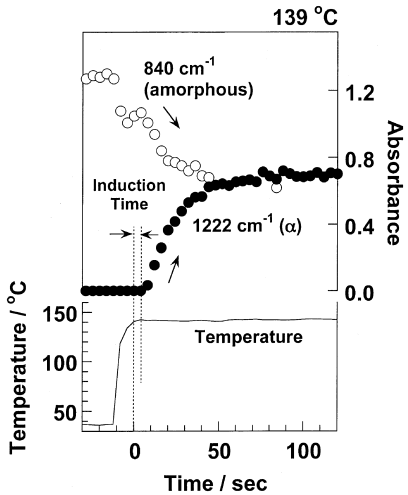

Fig. 7. Time dependence of infrared absorbance of the bands characteristic of the amorphous phase (840 cm^{-1}) and the α form (1222 cm^{-1}) measured in the isothermal crystallization at 139 °C.

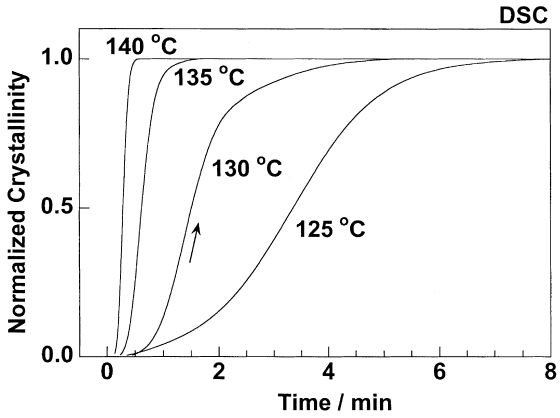

Fig. 8. Crystallization isotherms measured for sPS glass at the various temperatures of 125, 130, 135 and 140 °C.

kinds of data are consistent within the experimental error. That is to say, the macroscopically observed crystallization reflects exactly the microscopically occurring structural ordering process. The n and $\log k$ evaluated from these curves are shown in Fig. 10. These values depend on the crystallization temperature. Avrami index n is about 2–5. The rate constant k is 10^{-4}–10^{-1} s^{-1}. These values are found to correspond relatively well to those reported in Ref. [38] based on DSC data. (It should be noticed here that the definition of k is different between the present paper and the reference. The reference used the Avrami equation of $1 - X(t) = \exp(-k't^n)$ instead of Eq. (1). Therefore we have the relation of $\log k' = n \log k$. In the reference n was assumed to be constant 3, and so their experimental value of $k' = 10^{-9}$–10^{-6} s^{-1} corresponds to $k = 10^{-3}$–10^{-2} s^{-1} according to the definition of Eq. (1)). With a rise of crystallization temperature, the n value increased gradually from 2 to 5. If this isothermal crystallization is assumed to occur homogeneously in the melt-quenched glassy sample, then $n = 2$ suggests a rod-like growth from sporadically generated nuclei of the α form. If the crystallization is heterogeneous, then $n = 2$ suggests a growth of disc-like growth from already existing nuclei or dusts. The $n = 3$ suggests a disc-like growth (homogeneous crystallization) or a growth of spherulites (heterogeneous crystallization).

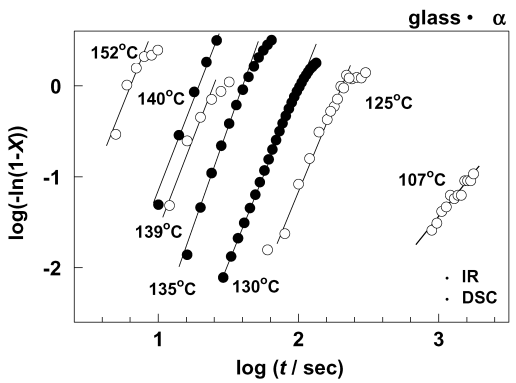

Fig. 9. Avrami plot made for the isothermal crystallization at the various temperatures. ○: infrared data and ●: DSC data.

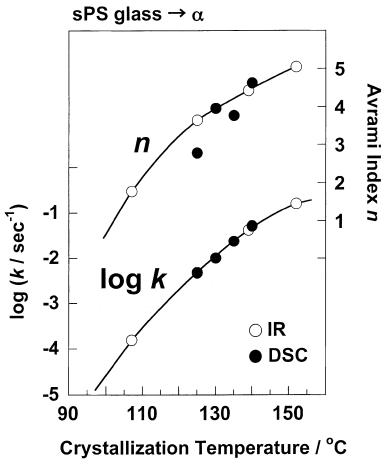

Fig. 10. Crystallization temperature dependence of Avrami index (n) and rate constant (k) estimated for the isothermal crystallization phenomenon of sPS glass. ○: infrared data and ●: DSC data.

The $n = 4$ suggests a homogeneous three-dimensional spherulitic growth. The heterogeneous crystallization with $n = 5$ is said to come from a three-dimensional cone-like spherulite growth [53] but it is not sure in the present study. We need to observe the morphological change by polarized optical microscope. Anyway, the increase of n from 2 to 5 with increasing crystallization temperature suggests a remarkable change of crystallization behavior.

The rate constant k can be expressed as having contributions from the two temperature-dependent processes, nucleation and growth. The temperature dependence of k is expressed in Eq. (3).

$$k(T) = k_o \exp(-U/[R(T - T_\infty)])\exp(-A/[T(T_m^o - T)]) \quad (3)$$

where the parameter U is an activation energy for transport of molecules across the nucleus surface, A is a constant related with the thermodynamic free energy for the formation of the critical size nucleus, and k_o is a constant [38,54]. The influence of diffusive process is represented by the term $\exp(-U/[R(T - T_\infty)])$, while the thermodynamic driving force is included in the term $\exp(-A/[T(T_m^o - T)])$. T_m^o is an equilibrium melting temperature and T_∞ is the temperature at which any molecular motion hypothetically ceases. For sPS the T_m^o was set equal to 551 K and T_∞ was 343 K, which was 30 K lower than T_g [38,54]. When the temperature is close to T_g, the mobility of the molecules is low enough that the overall crystallization rate is dominated by the diffusive process. Although the third term cannot be ignored of course, the k is insensitive to a minor change of A in this temperature region. Therefore it may be reasonably assumed that the parameter A is almost constant in the present experimental temperature region. Therefore, it is possible to determine U and k_o from Eq. (3) using assigned value $A = 1.2 \times 10^5$ K^2 [38], where the A value reported in reference [38] was 3.5×10^5 K^2 but it should be modified to one third because of the difference of the definition of k value as already pointed out in the preceding paragraph. The

thus evaluated U and k_o were 4.1 kJ/mol and 3.9×10^2 s^{-1}, respectively. These values are close to those reported in a reference based on the DSC data ($U = 4.3$–6.3 kJ/mol and $k_o = 10^1$–10^2 s^{-1} where their original values were divided by 3 based on the different definition of k value) [38].

In Fig. 10 we may notice that the k value decreases as the crystallization temperature is lowered. In the region of the glass transition temperature (T_g, ca. 100 °C) the k value is in an order of 10^{-5} s^{-1} or is as negligibly small as to be impossible to evaluate in a practical experiment. As known well the micro-Brownian motion of polymer chains is ceased below T_g and the crystallization does not occur actually in a normal time scale of hours to days. The negligibly small k value around the T_g corresponds to this situation. In other words, an extrapolation of the k value to the range of 10^{-5}–10^{-6} s^{-1} allows us to estimate the T_g from the viewpoint of crystallization kinetics.

3.2. Kinetics of solvent-induced crystallization

The sPS glass was exposed to organic solvent atmosphere at the various temperatures of 9–50 °C. Fig. 11(a) and (b) show the infrared spectral changes measured at 40 and 9 °C, respectively, during the solvent-induced crystallization process of sPS glass in the toluene atmosphere. The bands characteristic of the solvent and TTGG conformation were observed to increase in intensity, and the amorphous bands decreased in intensity after some induction time. Fig. 12 shows the time dependence of crystallinity estimated for the absorbance of 572 cm^{-1} infrared band characteristic of TTGG conformation. The critical sequence length of the band at 572 cm^{-1} is long, about 20–25 monomeric units or the 5–6 helical turns [22]. As reported before [19,21,22,25], the X-ray diffraction intensity started to increase almost in parallel to the intensity increment of the band with such a long critical sequence length. Therefore, the crystallinity

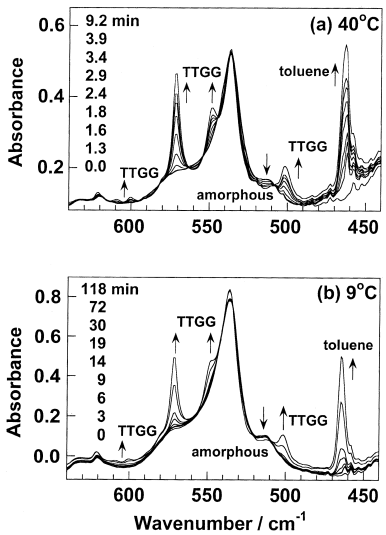

Fig. 11. Infrared spectral change of sPS glass exposed into the toluene atmosphere at (a) 40 and (b) 9 °C.

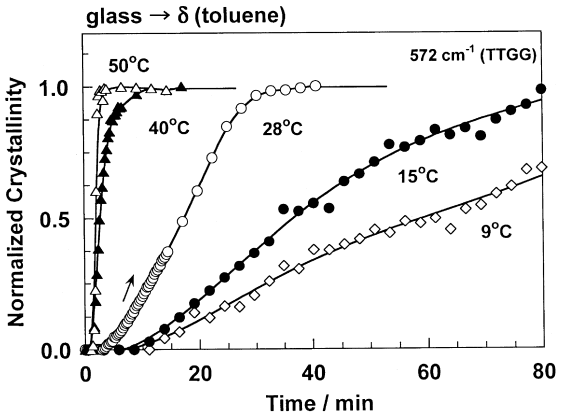

Fig. 12. Time dependence of normalized absorbance or crystallinity X estimated from the crystalline band intensity (572 cm^{-1}) measured for the sPS glass sample subjected to the toluene atmosphere at the various temperatures.

estimated from the 572 cm^{-1} band intensity may be used for the discussion of crystallization kinetics of the whole crystal lattice. The band intensity increased quite sharply when the experiment was made at 40–50 °C. The induction time was longer and the crystallization rate became lower as the crystallization temperature decreased to 15–9 °C. In this way the solvent-induced crystallization was found to be quite sensitive to the temperature as well as the kind of solvent [19,21,22,25].

Fig. 13 shows the Avrami plot using the data of Fig. 12. Here we need to mention about the complicatedness of the solvent-induced crystallization phenomenon. As easily speculated, the solvent molecules supplied from outside penetrate into the glass sample and diffuse into the central part. In the amorphous region invaded by the solvent molecules, nucleation of the δ form crystal starts to occur and the crystallites grow gradually. Since the solvent is supplied continuously the solvent molecules diffuse into deeper part of the glassy sample, where the nucleation and the crystal growth occur repeatedly. That is to say, the crystallization occurs heterogeneously over the whole sample as long as the sample thickness is not infinitesimally small. This is a quite different point from the case of

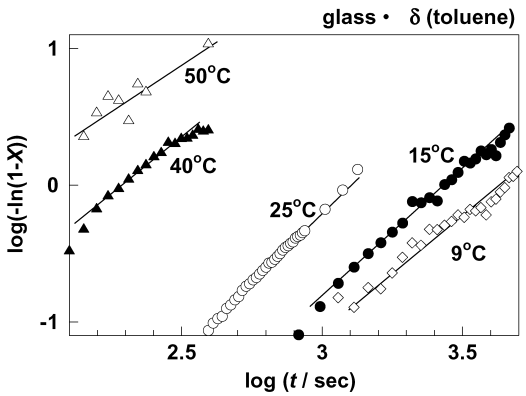

Fig. 13. Avrami plot for solvent-induced crystallization of sPS glass samples exposed to the toluene atmosphere at the various temperatures.

isothermal crystallization, in which the thermal energy is distributed homogeneously and the crystallization can be treated well on the basis of Avrami equation. In other words, the solvent-induced crystallization is not so simple as the isothermal crystallization and needs to be described in more complicated equation, for example, an equation derived from the convolution of the solvent diffusion phenomenon and the crystallization phenomenon. But, as will be reported elsewhere, such a convolution of the two kinds of phenomena gives a crystallization curve similar to the Avrami equation as long as an early stage of crystallization is focused on or in a low crystallinity region. Therefore the crystallization behavior observed in Fig. 12 may be described apparently in terms of Avrami equation as the first approximation. In fact, as seen in Fig. 13, the Avrami plot gives relatively good straight lines for the data collected at various temperatures. Of course the n and k values evaluated in this way might not have correct physical meanings but be only apparent. But, it is not perfectly incorrect to make a qualitative discussion by using these values.

The n value was about 1.7 ± 0.3 in the temperature region of 9–50 °C. The k value was in the range of 10^{-2} s^{-1} (50 °C) to 10^{-4} s^{-1} (9 °C) as shown in Fig. 14. Both of n and k values are apparently comparable to those estimated for the aforementioned isothermal crystallization phenomenon. As pointed out in the discussion about the isothermal crystallization of the α form, an extrapolation of k to the negligibly small value ($\sim 10^{-5}$) gives relatively reasonable T_g (see Fig. 14). A similar estimation was made also for the case of solvent-induced crystallization. As shown in Fig. 14, an extrapolation of log k to negligibly small value gives a temperature of ca. −15 °C. This temperature may be assumed as a glass transition temperature of sPS glass (T_g') attained by a plasticizing effect of absorbed solvent. As seen in Eq. (3), the k value consists of three terms of k_o, U and A. The absorbed solvent is speculated to affect these parameters more or less. As a trial these parameters were

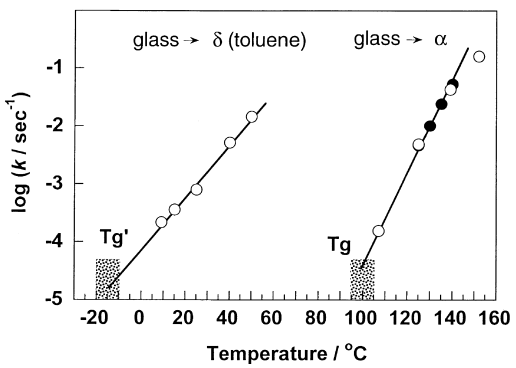

Fig. 14. Temperature dependence of the crystallization rate constant (k) obtained for the thermally induced crystallization from the glass to α form and the solvent-induced crystallization from the glass to δ from. T_g : the original glass transition temperature (ca. 100 °C) of sPS glass. T_g' (ca. −15 °C): the glass transition temperature estimated for the glass sample exposed in toluene atmosphere.

determined through the curve fitting procedure and we got $k_o = 3\ s^{-1}$, $U = 2.6$ kJ/mol, $A = 1.0 \times 10^4\ K^2$, $T_\infty = 214$ K and $T_m^o = 551$ K (fixed). Although we cannot compare these results directly with those obtained for the isothermal crystallization of the α form because of the different crystallization mechanism, the order of these parameters is appreciably low in the sPS–solvent system, reflecting the plasticizing effect on the molecular motion (k_o), transportation barrier (U) and formation energy (A). T_∞ is shifted from 343 to 214 K by ca. 130 K. This is consistent with the actually observed shift of T_g from 100 to −15 °C by about 115 °C as shown in Fig. 14, a quite large shift by a solvent (toluene) effect! It is well known that the T_g of nylon, for example, is reduced by about 50 °C when it absorbs water [55]. Therefore the decrement of T_g by ca. 115 °C is not impossible in the present case of sPS–toluene system. But this kind of discussion should be kept to a semiquantitative level, because the Avrami equation was applied only formally to the sPS–solvent system which should have quite complicated crystallization behavior coupled with a diffusion process of solvent molecules. More detailed treatment of this complicated crystallization behavior will be reported elsewhere.

4. Conclusions

In the present paper we discussed the kinetics of the thermally induced and solvent-induced crystallization phenomena of sPS glassy sample. The time-resolved infrared spectral measurement was made in the isothermal crystallization process from the glass to the α form and the induction time and crystallization rate were estimated. The time evolution of the crystallinity was analyzed on the basis of Avrami plot and the index n and the rate constant k were evaluated. The infrared and DSC data gave essentially the same results, i.e. the microscopically viewed structural change was found to reflect directly on the bulk thermal behavior.

In parallel the time-resolved measurement of infrared spectra was made for the first time for the solvent-induced crystallization process at various temperatures. The induction time and crystallization rate were found to change remarkably with temperature. The data analysis was made apparently on the basis of Avrami equation, although the actual crystallization behavior was considered to be more complicated. The thus estimated k value was found to change remarkably with temperature. An extrapolation of k to the negligibly small value allowed us to estimate a glass transition temperature of ca. −15 °C. That is, the plasticizing effect of absorbed solvent molecules was found to shift the T_g from ca. 100 °C of the original glassy sample to ca. −15 °C by 115 °C. Judging from the temperature dependence of the crystallization behavior shown in Figs. 12 and 14, this estimation seems reasonable. As mentioned above, the k value (and n value) might be only apparent because an

Avrami equation was applied to the system of complicated crystallization behavior. But, as long as the discussion is kept to the qualitative level, we may say that the unique solvent-induced crystallization phenomenon of sPS–solvent system has been understood relatively well from the kinetic point of view.

Acknowledgements

The authors wish to thank the Idemitsu Petrochemical Co., Ltd, Japan, for supplying sPS samples.

References

[1] Vittoria V, Russo R, de Candia F. Polymer 1991;32:3371.
[2] Vittoria V, Filho AR, de Candia F. Polym Bull 1991;26:445.
[3] Wang YK, Savage JD, Yang D, Hsu SL. Macromolecules 1992;25:3659.
[4] Chatani Y, Shimane Y, Inagaki T, Ijitsu T, Yukinari T, Shikuma H. Polymer 1993;34:1620.
[5] Chatani Y, Inagaki T, Shimane Y, Shikuma H. Polymer 1993;34:4841.
[6] De Candia F, Cartenuto M, Guadagno L, Vittoria VJ. Macromol Sci Phys 1996;B35:265.
[7] De Rosa C, Guerra G, Petraccone V, Pirozzi B. Macromolecules 1997;30:4147.
[8] Guerra G, Manfredi C, Musto P, Tavone S. Macromolecules 1998;31:1329.
[9] Moyses S, Sonntag P, Spells SJ, Laveix O. Polymer 1998;39:3537.
[10] Rastogi S, Goossens JGP, Lemstra PJ. Macromolecules 1998;31:2983.
[11] Guadagno L, Baldi P, Vittoria V, Guerra G. Macromol Chem Phys 1998;199:2671.
[12] Tsutsui K, Tsujita Y, Yoshimizu H, Kinoshita T. Polymer 1998;39:5177.
[13] Goossens H, Rastogi S, Lemstra P. Macromol Symp 1999;138:99.
[14] De Rosa C, Rizzo P, de Ballesteros OR, Petraccone V, Guerra G. Polymer 1999;40:2103.
[15] Tsutsui K, Katsumata T, Fukatsu H, Yoshimizu H, Kinoshita T, Tsujita Y. Polym J 1999;31:268.
[16] Tsutsui K, Katsumata T, Yamamoto Y, Fukatsu H, Yoshimizu H, Kinoshita T, Tsujita Y. Polymer 1999;40:3815.
[17] Moyses S, Spells SJ. Macromolecules 1999;32:2684.
[18] Moyses S, Spells SJ. Polymer 1999;40:3269.
[19] Tashiro K, Ueno Y, Yoshioka A, Kaneko F, Kobayashi M. Macromol Symp 1999;141:33.
[20] Musto P, Manzari M, Guerra G. Macromolecules 2000;33:143.
[21] Tashiro K, Sasaki S, Ueno Y, Yoshioka A, Kobayashi M. Korea Polym J 2000;8:103.
[22] Tashiro K, Ueno Y, Yoshioka A, Kobayashi M. Macromolecules 2001;34:310.
[23] Daniel C, Guerra G, Musto P. Macromolecules 2002;35:2243.
[24] van H-Corstjens CSJ, Magusin PCMM, Rastogi S, Lemstra PJ. Macromolecules 2002;35:6630.
[25] Tashiro K, Yoshioka A. Macromolecules 2002;35:410.
[26] Gowd EB, Nair SS, Ramesh C. Macromolecules 2002;35:8509.
[27] Milano G, Guerra G, M-Plathe F. Chemistry of materials 2002;14:2977.
[28] Mori S, Amutharani D, Yamamoto Y, Tsujita Y, Yoshimizu H. Polym Prepr Jpn 2002;51:2592.
[29] Tashiro K, Yoshioka A, Hashida T. Macromol Symp 2003; in press.
[30] Yoshioka A, Tashiro K. Polym Prepr Jpn 2002;51:2038.
[31] Naddeo C, Guadagno L, Aciemo D. Macromol Symp 1999;138:209.
[32] Reynolds NM, Stidham HD, Hsu SL. Macromolecules 1991;24:3662.
[33] Guerra G, Vitagliano VM, de Rosa C, Petraccone V, Corradini P. Macromolecules 1990;23:1539.
[34] De Rosa C, Guerra G, Petraccone V, Corradini P. Polym J 1991;23:1435.
[35] Sun Z, Miller RL. Polymer 1993;34:1963.
[36] Corradini P, de Rosa C, Guerra G, Napolitano R, Petraccone V, Pirozzi B. Eur Polym J 1994;30:1173.
[37] De Rosa C. Macromolecules 1996;29:8460.
[38] St Lawrence S, Shinozaki S, Polym DM. Eng Sci 1997;37:1825.
[39] Cartier L, Okihara T, Lotz B. Macromolecules 1998;31:3303.
[40] Woo EM, Sun YS, Lee ML. Polymer 1999;40:4425.
[41] De Rosa C, Rapacciuolo M, Guerra G, Petraccone V, de Corradini P. Polymer 1992;33:1423.
[42] Chatani Y, Shimane Y, Ijitsu T, Yukinari T. Polymer 1993;34:1625.
[43] Hamada N, Tosaka M, Tsuji M, Kohjiya S, Katayama K. Macromolecules 1997;30:6888.
[44] Tosaka M, Hamada N, Tsuji M, Kohjiya S. Macromolecules 1997;30:6592.
[45] Tosaka M, Hamada N, Tsuji M, Kohjiya S, Ogawa T, Isoda S, Kobayashi T. Macromolecules 1997;30:4132.
[46] Bu W, Li Y, He J, Zeng J. Macromolecules 1999;32:7224.
[47] Matsuda G, Kaji K, Nishida K, Kanaya T, Imai M. Macromolecules 1999;32:8932.
[48] Kobayashi M, Akita K, Tadokoro H. Makromol Chem 1968;118:324.
[49] Zhou S, Tashiro K, Hongo T, Shirataki H, Yamane C, Ii T. Macromolecules 2001;34:1274.
[50] Zhou S, Tashiro T, Ii T. Polym J 2001;33:344.
[51] Zhou S, Tashiro K, Ii T. J Polym Sci Polym Phys 2001;39:1638.
[52] Tashiro K, Sasaki S. Progr Polym Sci 2002;28:451.
[53] Mandelkern L. Crystallization of polymers. New York: McGraw-Hill; 1963.
[54] Wesson RD. Polym Engng Sci 1994;34:1157.
[55] Brandrup J, Immergut EH, Grulke EA, editors. Polymer handbook, 4th ed. New York: Wiley; 1999.